Am J Transl Res 2025;17(9):7146-7157
www.ajtr.org /ISSN:1943-8141/AJTR0166402

Original Article

Synergistic inhibition of glioblastoma by Furanodiene combined with Temozolomide and its immunological effects

Ying Chen[1], Yanhua Li[2], Tianfeng Liu[3], Linchun Huan[3], Xueyuan Heng[1]

[1]Guangzhou University of Chinese Medicine, Guangzhou 510006, Guangdong, China; [2]Shandong Medical College, Linyi 276000, Shandong, China; [3]Linyi People's Hospital, Linyi 276000, Shandong, China

Received May 28, 2025; Accepted August 20, 2025; Epub September 15, 2025; Published September 30, 2025

Abstract: Objective: To investigate the antitumor activity of the natural compound Furanodiene in glioblastoma multiforme (GBM), evaluate its synergistic effect with temozolomide (TMZ), and assess its potential to enhance antitumor immune responses. Methods: LN229 and U251 glioma cells, as well as patient-derived glioma stem-like cells (GSCs), were treated with Furanodiene alone or in combination with TMZ. Cell proliferation, apoptosis, and neurosphere formation were evaluated *in vitro*. For *in vivo* experiments, orthotopic glioma models were established in nude and C57BL/6 mice. Tumor burden was monitored via bioluminescence imaging, and survival was evaluated using the Kaplan-Meier analysis. Tumor sections were examined by immunofluorescence (Ki67, TUNEL), while immune responses were assessed via flow cytometry. Tumor rechallenge assays were performed to evaluate immune memory. Results: Furanodiene inhibited cell proliferation and induced apoptosis in a dose-dependent manner. Combined treatment with TMZ further enhanced cytotoxicity and suppressed neurosphere formation. *In vivo*, Furanodiene suppressed tumor growth, increased apoptosis, decreased Ki67 expression, and prolonged survival. Flow cytometry revealed increased $CD8^+$ T cell infiltration and TNF-α expression in tumor tissues. Rechallenge experiments confirmed resistance to tumor regrowth, indicating long-term immune memory. Conclusions: Furanodiene exerts potent antitumor effects and potentiates TMZ efficacy in GBM. Moreover, it enhances T cell activation and induces durable immune protection, supporting its potential as both a therapeutic and immunomodulatory agent.

Keywords: Glioblastoma, Furanodiene, Temozolomide, immunological effects, TNF-α, tumor microenvironment

Introduction

Glioblastoma (GBM) is one of the most aggressive and lethal primary brain tumors, characterized by rapid progression, high recurrence rates, and poor prognosis [1]. Despite advancements in standard-of-care treatments, including maximal surgical resection followed by radiotherapy and temozolomide (TMZ) chemotherapy, clinical outcomes remain unsatisfactory [2]. The median survival of most patients is less than 15 months, largely due to tumor recurrence and the development of drug resistance [3]. These limitations underscore an urgent need for novel treatment strategies.

In recent years, natural compounds derived from traditional Chinese medicine (TCM) have gained increasing attention for their anticancer potential. TCM compounds are known for their low toxicity, multi-target mechanisms, and a long history of clinical application in the diverse diseases [4-7]. Many TCM-based compounds have been shown to inhibit tumor progression, modulate immune system, and overcome drug resistance, making them promising candidates for adjuvant or combinatorial cancer therapies [8-10]. Mechanistically, various natural products exert their anticancer activity by inducing apoptosis, suppressing proliferation and metastasis, and reprogramming tumor cell metabolism [11, 12].

Furanodiene, a bioactive compound derived from Chinese herbs, has shown broad-spectrum antitumor activity across various cancers. It exerts anti-inflammatory, antioxidant, antiproliferative, pro-apoptotic, and anti-metastatic effects [13, 14]. Mechanistically, Furanodiene modulates key signaling pathways, including

https://doi.org/10.62347/GRSP1268

NF-κB, MAPK/ERK, and PI3K/Akt [15-17]. Preclinical studies have highlighted its ability to suppress tumor cell proliferation, inhibit angiogenesis, and induce cell cycle arrest in multiple cancer types, including hepatocellular carcinoma, lung cancer, breast cancer and leukemia [15, 18-21]. Furthermore, Furanodiene has been shown to reduce metastasis by interfering with epithelial-mesenchymal transition (EMT) and downregulating matrix metalloproteinases (MMPs), which are critical for tumor invasion [16, 22]. In addition to its direct tumor-inhibitory effects, Furanodiene also exhibits immunomodulatory properties. Importantly, its relatively low toxicity compared to conventional chemotherapeutic agents makes it an attractive candidate for long-term use or combination therapies [18].

Despite these promising properties, research on Furanodiene's application in brain tumors, particularly GBM, remains limited. The highly complex GBM microenvironment, coupled with the blood-brain barrier, poses significant challenges for effective drug delivery. Current findings are largely limited to *in vitro* studies, with little evidence regarding their *in vivo* efficacy, pharmacodynamics, and immunological impact in GBM models.

In this study, we systematically evaluated the antitumor activity of Furanodiene in GBM, both as a monotherapy and in combination with TMZ. Specifically, we investigated its effects on GBM cell proliferation, apoptosis, and neurosphere formation *in vitro*, and further assessed its antitumor efficacy, immune activation potential, and ability to induce long-term immune memory in mice models. Our goal is to explore Furanodiene's therapeutic potential in GBM and provide a theoretical foundation for its development for GBM treatment.

Methods

Cell culture

LN229 and GL261 cells were purchased from Shanghai Meiyan Biotechnology Co., Ltd., and U251 cells were obtained from the Cell Bank of the Chinese Academy of Sciences (Shanghai). Human glioma LN229 and U251 cell lines and murine-derived glioblastoma cell line GL261 were maintained in DMEM (Gibco, USA) supplemented with 10% fetal bovine serum (FBS; Gibco) and 1% penicillin/streptomycin solution. The cells were passaged using 0.25% trypsin/EDTA (Gibco).

Isolation and culture of patient-derived glioblastoma stem-like cells (GSCs)

Human glioblastoma specimens were obtained from patients treated at Linyi People's Hospital with informed consent and approval by the institutional ethics committee. Fresh GBM tumor tissues were transferred to HBSS medium immediately after resection, washed with PBS, minced into ~1 mm^3 fragments, and enzymatically digested with 1 mg/ml collagenase IV (Gibco, #17104-019) and 10 U/ml DNase I (Sigma-Aldrich, DN25) at 37°C for 20-30 minutes. Digestion was terminated by adding DMEM containing 10% FBS. The suspension was filtered through a 40 μm strainer, centrifuged, and resuspended in serum-free neural stem cell medium.

Low-passage GSCs were cultured as neurospheres in serum-free neurobasal medium (Gibco) supplemented with 1.5 × GlutaMAX (Gibco, #35050-061), 1 × B-27 (WISENT, #003-017-XL), 0.5 × N-2 (WISENT, #305-015-1L), 20 ng/mL EGF (PeproTech, #AF-100-15), and 20 ng/mL FGF (PeproTech, #AF-100-18B). Cells were maintained in low-attachment culture plates at 37°C with 5% CO_2 to promote neurosphere formation. Culture medium was partially refreshed every 3-5 days with fresh growth factors. For passaging, neurospheres were dissociated using the NeuroCult™ Chemical Dissociation Kit (STEMCELL Technologies, #05707), filtered, and re-seeded in fresh medium. For cryopreservation, neurospheres were collected, resuspended in BAMBANKER serum-free freezing medium (GC LYMPHOTEC, #302-14686), and stored at -80°C.

Cell viability

Cell viability was assessed using the CCK-8 assay kit. LN229 and U251 glioma cells were seeded in 96-well plates at a density of 5 × 10^3 cells per well and treated with Furanodiene (MedChemExpress) at concentrations of 50, 100, or 200 for 48 hours. For combination studies, cells were treated with 100 μM Furanodiene, 50 μM temozolomide (TMZ), or both for 48 hours. Following treatment, 10 μL of CCK-8 reagent (Beyotime, #C0039) was

added to each well and incubated at 37°C for 1-4 hours. Absorbance was measured at 450 nm using a microplate reader.

Neurosphere formation assay

Patient-derived GSCs were cultured as neurospheres in serum-free medium and dissociated into single cells using the NeuroCult™ Chemical Dissociation Kit. Single-cell suspensions were seeded into ultra-low attachment 96-well plates at a density of 1-2 × 10^4 cells per well. GSCs were treated with Furanodiene (100 or 200 μM), TMZ (50 μM), or their combination for 72 h. Neurosphere growth was monitored using the IncuCyte live-cell imaging system, and representative images were acquired at the endpoint. Neurosphere sizes were quantified using ImageJ software.

Cell death

Cells were harvested and washed three times with cold PBS. After centrifugation, the cell pellet was incubated with FITC Annexin V and PI (Sigma) staining at room temperature for 15 minutes, followed by analysis using flow cytometry.

Immunofluorescence

GBM tissues were fixed in 4% paraformaldehyde (PFA) overnight at 4°C, followed by dehydration in 30% sucrose for 24 h. Samples were embedded in OCT compound, sectioned at 10 μm thickness, and fixed in acetone for 10 min at -20°C. Tissue sections were permeabilized with 0.5% Triton-X 100 in PBS for 10 min and blocked with 5% BSA for 1 h at room temperature. Slides were then incubated overnight at 4°C with primary antibody against Ki67 (Abcam, ab16667, 1:200 dilution). After washing with PBS, sections were incubated with secondary antibodies (Invitrogen, #A-11034; 1:500 dilution) at room temperature for 2 h. Finally, nuclei were counterstained with DAPI solution and mounted with antifade mounting medium.

Animal experiments

Human glioma LN229 and murine GL261 glioma cells were transfected with a lentiviral vector encoding firefly luciferase (Fluc). LN229 cells (1 × 10^6) or GL261 cells (1 × 10^5) expressing Fluc were stereotactically injected into the striatum of 6- to 8-week-old female C57BL/6 or nu/nu mice (coordinates relative to bregma: 2.0 mm anterior-posterior (AP), 2.0 mm mediolateral (ML), and 3.0 mm dorso-ventral (DV)). A single bilateral intracerebroventricular injection (5 μL per side) of Furanodiene (10 mg/kg per mouse) was administered at a flow rate of 500 nL/min. The injection coordinates relative to bregma were: 0.3 mm AP, ±0.7 mm ML, and 3.0 mm DV. Temozolomide (TMZ, TCI America, Catalog #T2744) was dissolved in DMSO and administered via oral gavage at 25 mg/kg, for five consecutive days per week.

Tumor growth was monitored using an in vivo imaging system (IVIS). For survival studies, mice were euthanized upon signs of morbidity, including hunching posture and significant weight loss. In rechallenge experiments, mice that survived initial Furanodiene treatment were age-matched with naïve C57BL/6 control mice (n = 3 per group) and orthotopically re-injected with 1 × 10^5 GL261 cells. All mice were euthanized by carbon dioxide (CO_2) inhalation at a high flow rate in a sealed chamber until loss of consciousness and complete cessation of respiration and heartbeat. The gas flow was maintained for at least one additional minute to ensure death, followed by cervical dislocation. All animal procedures were approved by the Science Research Ethics Committee of Linyi People's Hospital (Ethics No: YX200634).

TUNEL staining

Apoptotic cells in intracranial tumor tissues were detected using the TUNEL (terminal deoxynucleotidyl transferase dUTP nick-end labeling) assay. Brain tissues were harvested from tumor-bearing mice, fixed in 4% PFA overnight at 4°C, and dehydrated in 30% sucrose for 24 hours. The tissues were then embedded in OCT compound, sectioned at 10 μm thickness, and fixed in cold acetone for 10 minutes at -20°C. TUNEL staining was performed using the In Situ Cell Death Detection Kit (Roche, #11684817910) according to the manufacturer's instructions. Briefly, sections were permeabilized with proteinase K (diluted in TE buffer (10 mM Tris-HCl, 1 mM EDTA, pH 8.0)) and 0.2% Triton X-100 sequentially in PBS. Slides were then incubated with the TUNEL reaction mixture at 37°C for 60 minutes in a humidified

chamber, followed by nuclear counterstaining with DAPI. Images were acquired using a fluorescence microscope.

Flow cytometry assay

Intracranial tumor tissues were harvested from GL261-bearing C57BL/6 mice following Furanodiene or vehicle treatment. Brains were rapidly dissected, and visible tumor regions were isolated under a stereomicroscope. Tumor samples were minced into small fragments and passed through a 70 μm cell strainer to obtain a single-cell suspension. The suspension was digested using a solution containing 1.5 mg/mL collagenase and 20 μg/mL DNase in HBSS at 37°C for 30 minutes. After digestion, cells were collected and treated with RBC lysis buffer to remove red blood cells, followed by pretreatment with an Fc-blocking antibody (CD16/CD32, BD Biosciences, #553142) at 4°C for 15 minutes to prevent nonspecific binding. Then cells were resuspended in flow buffer (2% FBS in PBS) and incubated with CD45 (APC-conjugated anti-mouse, BD Biosciences, #559864, 1:100 dilution), CD3 (PE-conjugated anti-mouse, BD Biosciences, #555275, 1:100 dilution) and CD8 (FITC-conjugated anti-mouse, BD Biosciences, 561966, 1:100 dilution) antibodies at room temperature for 1h. To assess cytokine expression, cells were resuspended in DMEM medium containing 10% FBS and 1% penicillin/streptomycin, and then activated with Leukocyte Activation Cocktail (BD Biosciences, #554656; 1:100 dilution) at 37°C for 6 hours. Following activation, the cells were stained with a TNF antibody (BV421-conjugated anti-mouse, BD Biosciences, #563387). Flow cytometric analysis was performed using a BD Biosciences flow cytometer, and the resulting data were processed with FlowJo software.

Data analysis

Quantitative data were analyzed using GraphPad Prism 10.0 software. Results were presented as mean ± standard error of the mean (SEM). Statistical comparisons between two groups were conducted using unpaired two-tailed Student's t-tests, while multiple-group comparisons were conducted using one-way ANOVA. Survival data were analyzed using the Kaplan-Meier method and compared using the log-rank (Mantel-Cox) test. A p-value < 0.05 was considered statistically significant.

Results

Inhibitory effect of Furanodiene on glioma cell and glioma stem-like cells (GSCs)

This study investigated the inhibitory effects of Furanodiene on the proliferation and survival of glioma cells and GSCs. Human glioma cell lines LN229 and U251 were treated with increasing concentrations of Furanodiene (50-200 μM). LN229 cells are TMZ-sensitive due to MGMT promoter methylation, whereas U251 cells are TMZ-resistant owing to its unmethylated promoter [23, 24]. These two models allowed us to assess the efficacy of Furanodiene across different molecular subtypes of glioma.

CCK-8 assays revealed a significant, dose-dependent reduction in proliferation of both LN229 and U251 cells following Furanodiene treatment (**Figure 1A**, **1B**). Flow cytometry further demonstrated that Furanodiene markedly increased cell death, with 200 μM inducing significantly more apoptosis than 100 μM ($P < 0.001$; **Figure 1C**). In addition, Furanodiene treatment significantly inhibited the sphere-forming capacity of patient-derived GSCs in a concentration-dependent manner ($P < 0.01$; **Figure 1D**). Collectively, these results indicate that Furanodiene effectively suppresses proliferation and promotes cell death in both glioma cells and GSCs, highlighting its potential as a therapeutic agent against aggressive GBM.

Enhanced inhibition by combined Furanodiene and TMZ treatment in GBM cells

TMZ remains the standard chemotherapeutic agent for GBM treatment; however, its efficacy is often compromised in tumors with unmethylated MGMT promoters, which confer resistance by repairing TMZ-induced DNA damage [25]. To investigate whether Furanodiene could potentiate TMZ efficacy, we explored the therapeutic effects of their combination in GBM models.

CCK-8 assay showed that combined treatment more strongly suppressed proliferation of both LN229 and U251 cells compared with Furanodiene or TMZ alone, demonstrating a synergistic effect ($P < 0.0001$; **Figure 2A**, **2B**). Flow cytometry further revealed a marked increase in cell death in the combination group, suggesting enhanced cytotoxicity ($P < 0.01$; **Figure 2C**). Additionally, the sphere formation assay further

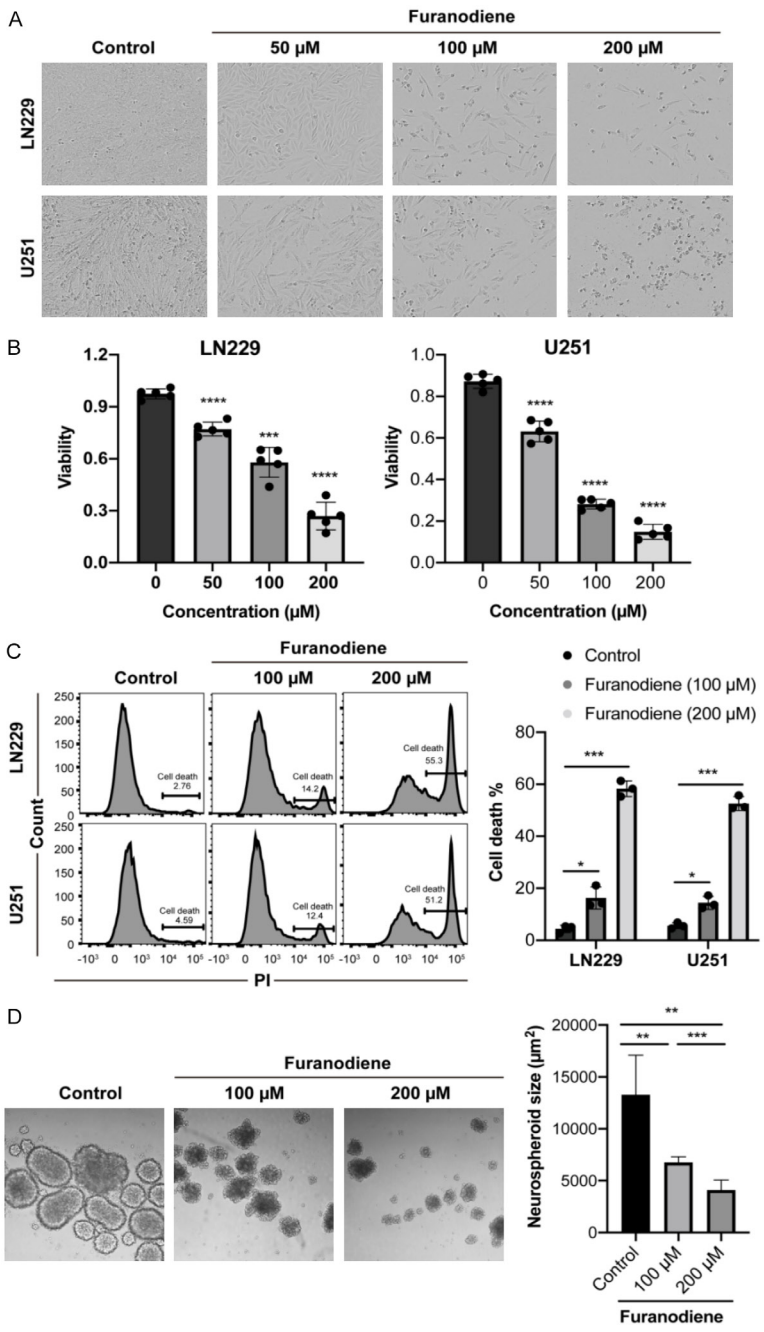

Figure 1. Inhibitory effect of Furanodiene on glioma and GBM cell proliferation. A. LN229 and U251 cells were exposed to varying concentrations of Furanodiene (50, 100, and 200 μM) for 48 hours, with representative bright-field images displayed. B. Cell proliferation was assessed using the CCK8 assay after treatment with Furanodiene (50, 100, and 200 μM) for 48 hours, showing significant suppression in both LN229 and U251 cells. C. LN229 and U251 cells treated with 100 and 200 μM Furanodiene for 48 hours were analyzed for cell death using PI staining and flow cytometry. D. Patient-derived glioblastoma GSCs were treated with 100 and 200 μM Furanodiene for 3 days. Bright-field images and quantification of neurosphere sizes demonstrated notable inhibition. **P < 0.01; ***P < 0.001; ****P < 0.0001.

showed that the combination of Furanodiene and TMZ significantly inhibited the neurosphere formation ability of GSCs relative to monotherapies, highlighting its potential to target stem cell-like tumor populations (P < 0.0001; **Figure 2D**). Collectively, these findings provide compelling experimental evidence that Furanodiene enhances the antitumor efficacy of TMZ, supporting its potential as a synergistic therapeutic agent for GBM.

Enhanced antitumor activity of Furanodiene and TMZ combination therapy in a nude mouse glioma model

To further investigate the antitumor efficacy of Furanodiene *in vivo*, an intracranial glioma model was established by stereotactic implantation of Fluc-labeled LN229 cells into nude mice. Once tumors reached a measurable size, Furanodiene was administered via intracerebroventricular injection starting on day 20, repeated every 10 days for a total of four treatments. In the combination group, TMZ was administered orally following a 5-day-on/2-day-off regimen for three consecutive weeks (**Figure 3A**). Furanodiene monotherapy significantly reduced tumor growth compared to vehicle-treated controls, while the combination with TMZ further suppressed tumor burden, suggesting a synergistic effect (**Figure 3B**, **3C**). Immunohistochemical staining revealed a marked decrease in Ki67-positive proliferating cells in both the Furanodiene and combination groups, with the most pronounced decrease observed under combination treatment (**Figure 3D**). TUNEL staining further confirmed that both treatments enhanced tumor cell apoptosis, with a higher proportion

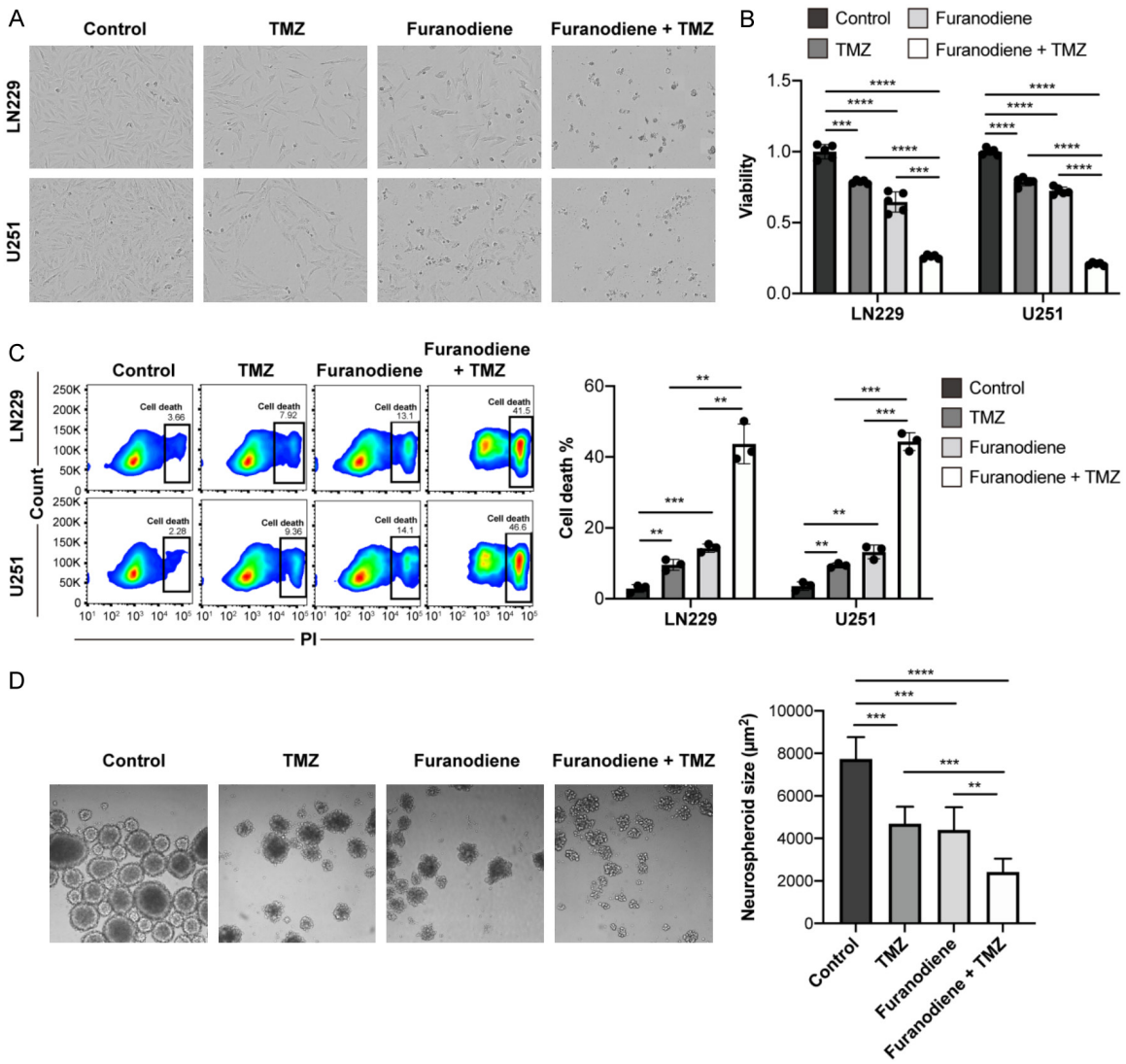

Figure 2. Enhanced inhibition of gliomas by combination therapy of Furanodiene and TMZ. A. LN229 and U251 cells were treated with 100 μM Furanodiene, 50 μM TMZ, or their combination for 48 hours. Representative bright-field images are shown. B. The combined treatment significantly reduced cell proliferation, as measured by the CCK8 assay. C. Flow cytometry analysis of LN229 and U251 cells treated with 100 μM Furanodiene, 50 μM TMZ, or their combination revealed increased PI-stained cell death. D. Patient-derived glioblastoma GSCs were treated with 100 μM Furanodiene, 50 μM TMZ, or both for 3 days. Bright-field images and neurosphere size quantification highlighted enhanced inhibition with the combination therapy. **P < 0.01; ***P < 0.001; ****P < 0.0001.

of TUNEL-positive cells observed in the combination group compared to monotherapies (**Figure 3E**). K-M survival analysis demonstrated that Furanodiene significantly prolonged overall survival compared with controls, and the combination therapy showed the most substantial survival benefit among all groups (**Figure 3F**). Collectively, these findings indicate that Furanodiene exerts potent antitumor effects *in vivo* and that its combination with TMZ enhances therapeutic efficacy in glioma-bearing mice.

Antitumor effects of Furanodiene in an immunocompetent mouse glioma model

To assess the antitumor efficacy of Furanodiene in an immunocompetent context, an orthotopic glioma model was established by stereotactica implantation of Fluc-labeled, mouse-derived GL261 glioblastoma cells into the brains of C57BL/6 mice. Following tumor establishment, Furanodiene was administered via intracerebroventricular injection. Compared to vehicle-treated controls, Furanodiene treatment signifi-

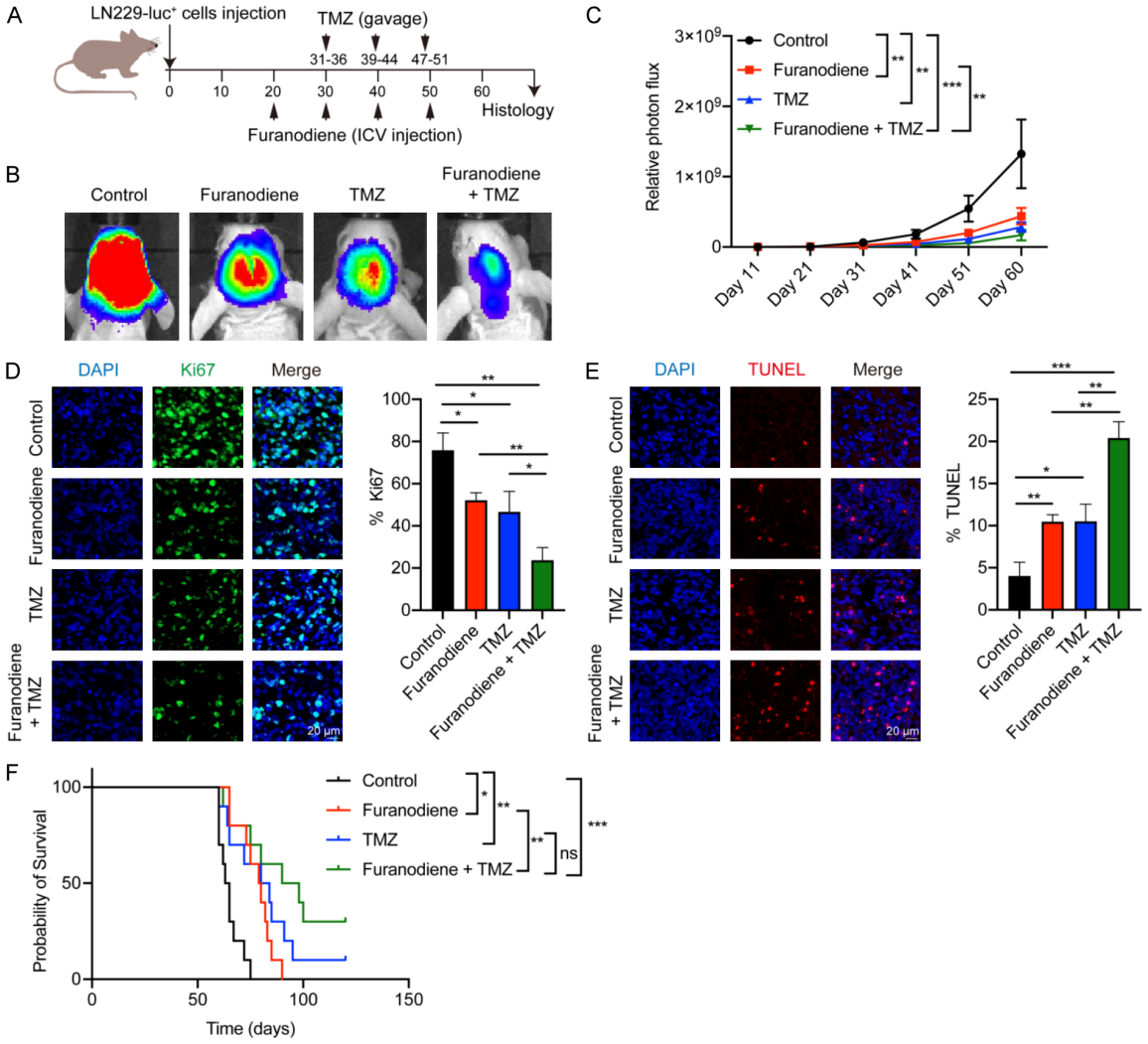

Figure 3. Anti-tumor effects of Furanodiene and TMZ combination therapy in a nude mouse glioma model. A. Human glioma LN229 cells (1×10^6) expressing firefly luciferase were stereotactically injected into the striatal region of 6-week-old nu/nu mice. Bilateral intracerebroventricular injections (5 μl per side) of Furanodiene were administered on days 20, 30, and 40 after LN229 cell injections. TMZ (25 mg/kg) was given via gavage on Days 31-36, 39-44, and 47-51. B, C. Tumor burden was evaluated by measuring luminescence signals using a luciferase imaging system. D. Tumor proliferative index was assessed through Ki67 immunostaining, with representative images shown (left), and the percentage of Ki67-positive cells quantified (right) for each group. E. Apoptosis was analyzed via TUNEL staining, with representative images displayed (left), and the percentage of TUNEL-positive cells quantified (right) across groups. F. Survival data for mice across all tumor groups are presented. ns, not significant; *P < 0.05; **P < 0.01; ***P < 0.001.

cantly suppressed tumor growth, as demonstrated by bioluminescence imaging (**Figure 4A-C**). Histological examination revealed a marked reduction in Ki67 expression, indicating decreased tumor cell proliferation (**Figure 4D**), together with a significant increase in TUNEL-positive cells, reflecting enhanced apoptosis (**Figure 4E**). Survival analysis further showed that Furanodiene significantly prolonged overall survival, with approximately 30% of treated mice achieving long-term survival (**Figure 4F**). These findings demonstrate that Furanodiene exerts potent antitumor activity in an immunocompetent glioma model and support its potential as a candidate for further preclinical development in GBM therapy.

Furanodiene-induced T cell activation and immune memory formation

To investigate whether Furanodiene exerts its antitumor effects through immune activation,

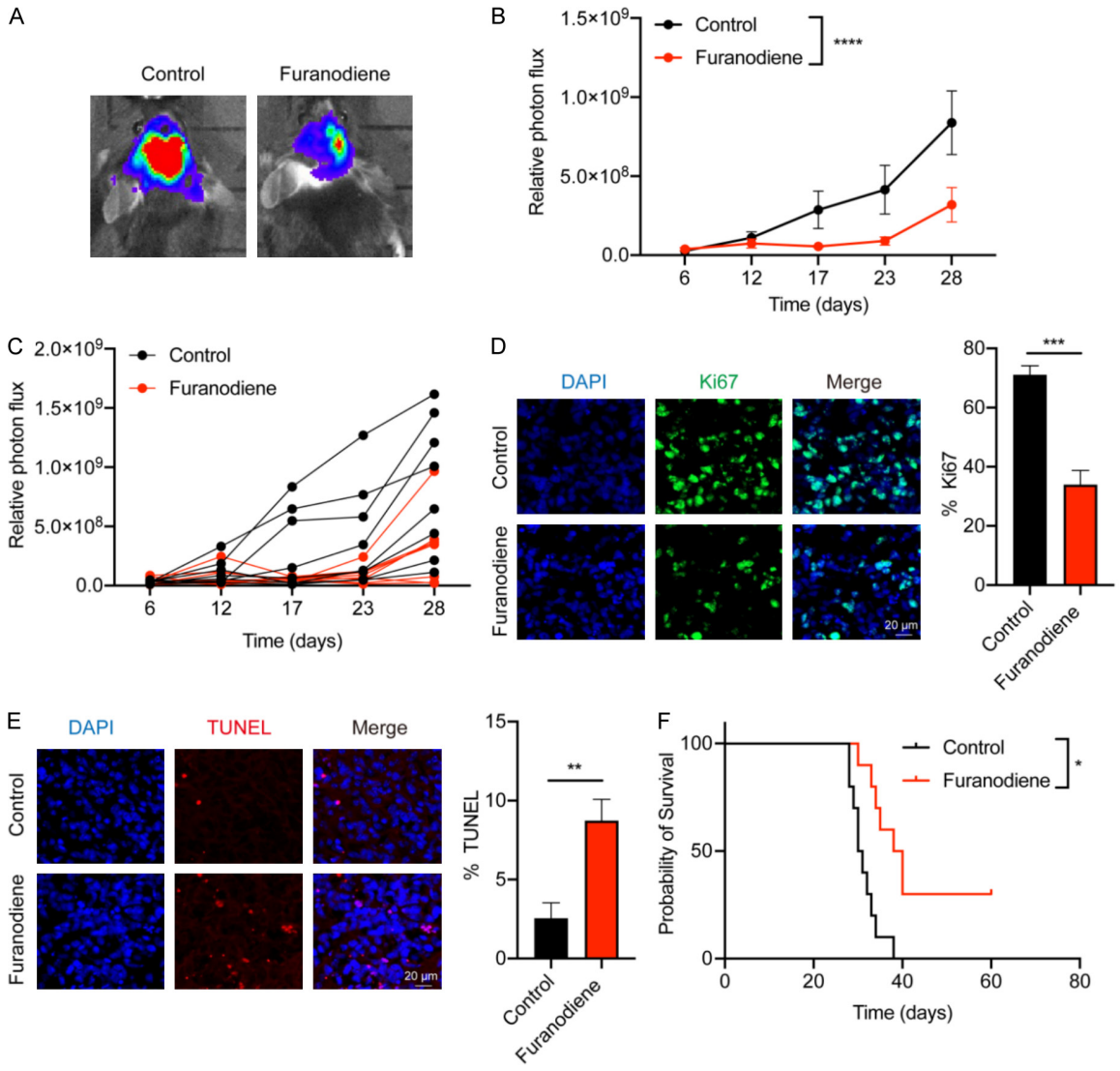

Figure 4. Antitumor effects of Furanodiene in an immunocompetent mouse glioma model. (A) GL261 cells (1×10^5) expressing firefly luciferase were stereotactically injected into the striatal region of 6-8-week-old C57BL/6 female mice. Bilateral intracerebroventricular injections (5 μl per side) of Furanodiene were administered on days 7, 14, and 21 post-injections. Representative luminescence images from control (DMSO) and Furanodiene-treated mice on day 28 are displayed. (B, C) Tumor growth is shown as the average luminescence per group (B), and individual tumor growth for each animal (C). (D) Immunostaining results of tumor proliferative index Ki67, with representative images displayed (left) and the percentage of Ki67-positive cells quantified (right) for each group. (E) Apoptosis was evaluated via TUNEL staining, with representative images shown (left), and the percentage of TUNEL-positive cells quantified (right) across groups. (F) Survival data for all tumor groups are presented. ns, no significance; *P < 0.05; **P < 0.01; ***P < 0.001; ****P < 0.0001.

particularly via T cells, we analyzed tumor-infiltrating lymphocytes in GL261-bearing mice with flow cytometry. Compared to the control group, Furanodiene-treated tumors exhibited significantly higher infiltration of immune cells ($CD45^+$) and T cells ($CD3^+$, $CD8^+$), along with elevated expression of the activation marker TNF-α (**Figure 5A-C**), indicating robust T cell activation within the tumor microenvironment.

To further evaluate the potential for immune memory formation, we conducted tumor rechallenge experiments by re-injecting GL261 cells into mice that had survived initial Furanodiene treatment (**Figure 5D**). While all naïve control mice developed tumors, previously treated mice showed complete resistance to tumor regrowth, suggesting the establishment of durable antitumor immune memory. Collectively,

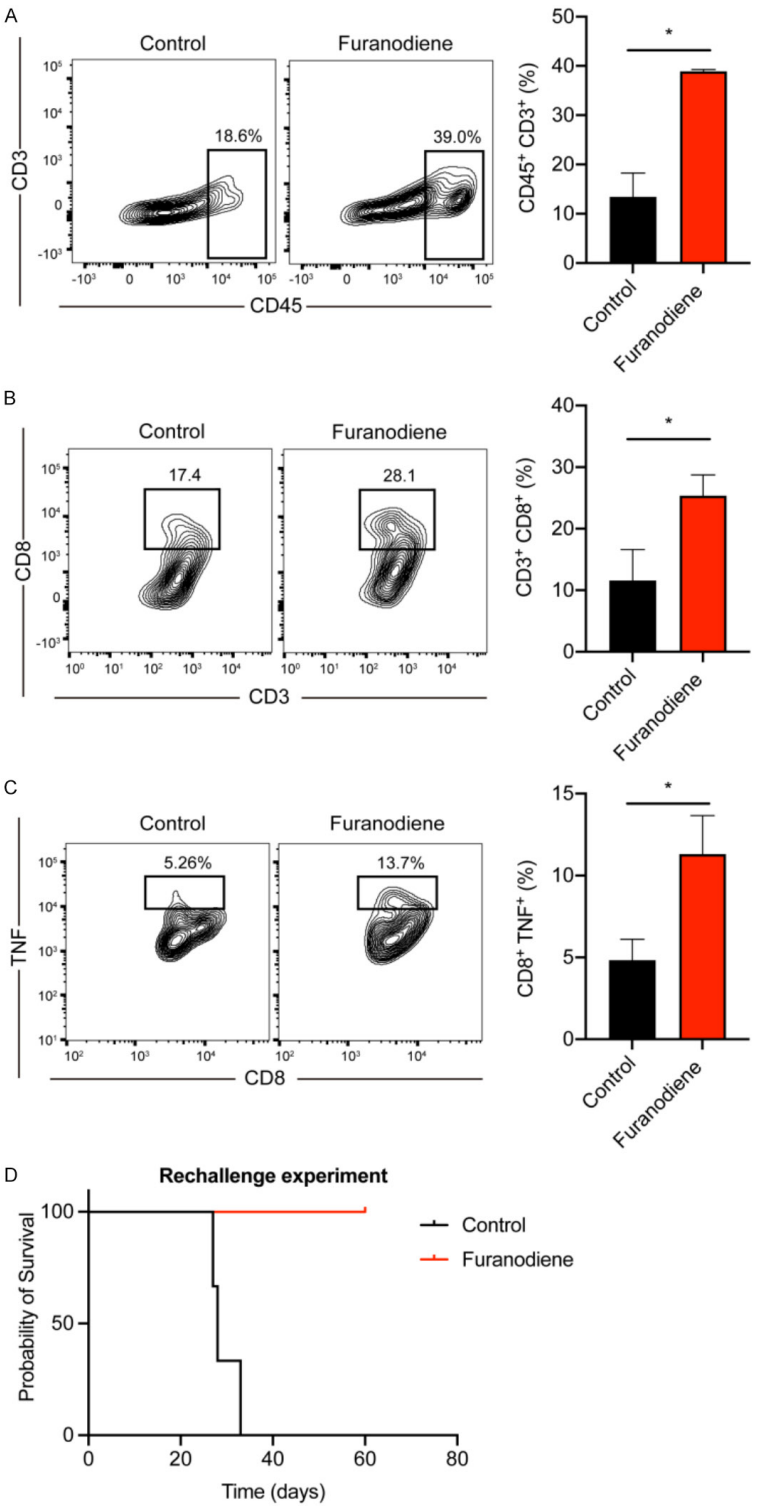

Figure 5. Furanodiene-induced T cell activation and immune memory formation. A-C. Flow cytometric analysis of T cell (CD3+, CD8+) infiltration as well as TNF-α expression in GL261-bearing mice following Furanodiene treatment. D. Mice survived initial Furanodiene treatment displayed notably higher survival rate compared to age-matched naïve C57BL/6 mice (n = 3/group) after tumor rechallenge. *P < 0.05.

these results demonstrate that Furanodiene not only promotes T cell-mediated antitumor responses but also facilitates long-term immune protection, highlighting its potential as a novel immunomodulatory agent in glioblastoma therapy.

Discussion

GBM remains one of the most challenging malignancies in oncology due to its aggressive progression, diffuse infiltration, and resistance to conventional therapies [1, 2]. The intrinsic heterogeneity of GBM and its capacity to invade surrounding brain tissue make complete surgical resection nearly impossible, often resulting in recurrence [26-28]. Moreover, temozolomide (TMZ), the current standard chemotherapeutic agent, frequently encounters resistance due to enhanced DNA repair mechanisms, most notably O6-methylguanine-DNA methyltransferase (MGMT), which effectively reverses TMZ-induced DNA lesions [25]. These clinical obstacles highlight the urgent need for novel therapeutic strategies that address the multifactorial resistance mechanisms in GBM.

Furanodiene, a sesquiterpenoid extracted from *Curcuma wenyujin*, exhibits broad antitumor activity through its multitarget pharmacological profile [13, 14]. Distinct from traditional chemotherapeutics that act on a single molecular target, Furanodiene modulates several key oncogenic signaling pathways, including NF-κB, MAPKs, and Akt [15-17]. These pathways are criti-

cal regulators of cancer cell survival, proliferation, and metastasis, and their inhibition leads to tumor cell apoptosis, reduced angiogenesis, and suppression of metastasis [15, 22, 29-31]. Our results demonstrate that Furanodiene significantly inhibits GBM cell proliferation and induces apoptosis, in both cell culture and patient-derived neurosphere models, suggesting its effectiveness against GSCs, which play a critical role in therapy resistance and tumor recurrence.

Furanodiene has also shown strong synergistic effects when combined with various chemotherapeutic agents in preclinical studies. For instance, it enhances the antitumor activity of 5-fluorouracil (5-FU) in breast and liver cancer models [32], and sensitizes adriamycin-resistant breast cancer cells by modulating mitochondrial function via AMPK signaling, thereby restoring drug sensitivity even in ERα-deficient cells [17, 18]. In lung cancer models, Furanodiene potentiates the effects of paclitaxel (TAX), likely through modulation of cell cycle regulators and induction of mitochondrial dysfunction, leading to enhanced cytotoxicity [33]. Furthermore, in multidrug-resistant tumor models, Furanodiene effectively reverses drug resistance, including cisplatin-resistant non-small cell lung cancer and adriamycin-resistant breast cancer [32]. These findings support Furanodiene's potential to overcome therapeutic resistance through diverse, complementary mechanisms.

Consistent with these observations, our study further revealed that Furanodiene combined with TMZ demonstrated superior antitumor effects compared to either treatment alone. TMZ exerts its cytotoxic effect by inducing DNA alkylation and subsequent apoptosis [25], but its efficacy is often compromised in tumors with high MGMT expression or enhanced DNA repair capacity [25, 34]. In our GBM models, the combination of Furanodiene and TMZ exhibited significantly enhanced antiproliferative and pro-apoptotic effects compared to either agent alone. This synergistic interaction is likely attributable to their complementary mechanisms of action. TMZ primarily exerts its antitumor effect by inducing DNA damage, whereas Furanodiene disrupts key pro-survival signaling pathways, inducing NF-κB, MAPKs, and Akt [15-17], which are frequently upregulated in GBM and contribute to treatment resistance. Furthermore, Furanodiene also targets GSCs, as indicated by its inhibition of neurosphere formation, thereby addressing a major limitation of TMZ monotherapy, which often fails to eradicate this resistant subpopulation. The combination therapy not only reduced proliferation markers such as Ki67 but also increased apoptosis as evidenced by TUNEL staining, providing compelling support for the therapeutic synergy between Furanodiene and TMZ in GBM models.

Beyond its cytotoxic properties, Furanodiene also stimulated antitumor immunity. Our results showed increased infiltration of $CD8^+$ T cells and elevated TNFα expression in Furanodiene-treated tumors. Furthermore, mice that responded to initial Furanodiene treatment exhibited long-term immune memory upon tumor rechallenge. These findings suggest that Furanodiene not only suppresses tumor growth directly but may also enhance the host's immune surveillance, offering a dual mechanism of action.

In summary, Furanodiene holds promise as both a monotherapy and an adjuvant to TMZ in GBM. By inhibiting oncogenic pathways, overcoming chemoresistance, targeting GSCs, and enhancing antitumor immunity, Furanodiene offers a compelling strategy for combination therapy. Although further studies are warranted to optimize dosing regimens, elucidate precise mechanisms, and evaluate clinical applicability, our findings support Furanodiene's potential as a novel therapeutic candidate in the management of GBM.

Disclosure of conflict of interest

None.

Address correspondence to: Xueyuan Heng, Guangzhou University of Chinese Medicine, Guangzhou 510006, Guangdong, China. Tel: +86-13290209866; E-mail: rmyy13854909710@163.com

References

[1] Omuro A and DeAngelis LM. Glioblastoma and other malignant gliomas: a clinical review. JAMA 2013; 310: 1842-1850.
[2] Schaff LR and Mellinghoff IK. Glioblastoma and other primary brain malignancies in adults: a review. JAMA 2023; 329: 574-587.

[3] Obrador E, Moreno-Murciano P, Oriol-Caballo M, Lopez-Blanch R, Pineda B, Gutierrez-Arroyo JL, Loras A, Gonzalez-Bonet LG, Martinez-Cadenas C, Estrela JM and Marques-Torrejon MA. Glioblastoma therapy: past, present and future. Int J Mol Sci 2024; 25: 2529.
[4] Zhang X, Qiu H, Li C, Cai P and Qi F. The positive role of traditional Chinese medicine as an adjunctive therapy for cancer. Biosci Trends 2021; 15: 283-298.
[5] Xiang Y, Guo Z, Zhu P, Chen J and Huang Y. Traditional Chinese medicine as a cancer treatment: modern perspectives of ancient but advanced science. Cancer Med 2019; 8: 1958-1975.
[6] Miao K, Liu W, Xu J, Qian Z and Zhang Q. Harnessing the power of traditional Chinese medicine monomers and compound prescriptions to boost cancer immunotherapy. Front Immunol 2023; 14: 1277243.
[7] Zhang Y, Lou Y, Wang J, Yu C and Shen W. Research status and molecular mechanism of the traditional Chinese medicine and antitumor therapy combined strategy based on tumor microenvironment. Front Immunol 2020; 11: 609705.
[8] Wang J, Qi F, Wang Z, Zhang Z, Pan N, Huai L, Qu S and Zhao L. A review of traditional Chinese medicine for treatment of glioblastoma. Biosci Trends 2020; 13: 476-487.
[9] Efferth T, Schottler U, Krishna S, Schmiedek P, Wenz F and Giordano FA. Hepatotoxicity by combination treatment of temozolomide, artesunate and Chinese herbs in a glioblastoma multiforme patient: case report review of the literature. Arch Toxicol 2017; 91: 1833-1846.
[10] Cao H, Li X, Wang F, Zhang Y, Xiong Y and Yang Q. Phytochemical-mediated glioma targeted treatment: drug resistance and novel delivery systems. Curr Med Chem 2020; 27: 599-629.
[11] Wang S, Fu JL, Hao HF, Jiao YN, Li PP and Han SY. Metabolic reprogramming by traditional Chinese medicine and its role in effective cancer therapy. Pharmacol Res 2021; 170: 105728.
[12] Zhang Y, Fang F, Fan K, Zhang Y, Zhang J, Guo H, Yu P and Ma J. Effective cytotoxic activity of OSW-1 on colon cancer by inducing apoptosis in vitro and in vivo. Oncol Rep 2017; 37: 3509-3519.
[13] Batool R, Rasul A, Hussain G, Shah MA, Nageen B, Sarfraz I, Zahoor MK, Riaz A, Ajaz A and Adem S. Furanodiene: a novel, potent, and multitarget cancer-fighting terpenoid. Curr Pharm Des 2021; 27: 2628-2634.
[14] Lu JJ, Dang YY, Huang M, Xu WS, Chen XP and Wang YT. Anti-cancer properties of terpenoids isolated from Rhizoma Curcumae--a review. J Ethnopharmacol 2012; 143: 406-411.
[15] Zhong ZF, Yu HB, Wang CM, Qiang WA, Wang SP, Zhang JM, Yu H, Cui L, Wu T, Li DQ and Wang YT. Furanodiene induces extrinsic and intrinsic apoptosis in doxorubicin-resistant MCF-7 breast cancer cells via NF-kappaB-independent mechanism. Front Pharmacol 2017; 8: 648.
[16] Zhong Z, Tan W, Chen X and Wang Y. Furanodiene, a natural small molecule suppresses metastatic breast cancer cell migration and invasion in vitro. Eur J Pharmacol 2014; 737: 1-10.
[17] Zhong ZF, Tan W, Qiang WW, Scofield VL, Tian K, Wang CM, Qiang WA and Wang YT. Furanodiene alters mitochondrial function in doxorubicin-resistant MCF-7 human breast cancer cells in an AMPK-dependent manner. Mol Biosyst 2016; 12: 1626-1637.
[18] Zhong ZF, Qiang WA, Wang CM, Tan W and Wang YT. Furanodiene enhances the anti-cancer effects of doxorubicin on ERalpha-negative breast cancer cells in vitro. Eur J Pharmacol 2016; 774: 10-19.
[19] Zhong Z, Dang Y, Yuan X, Guo W, Li Y, Tan W, Cui J, Lu J, Zhang Q, Chen X and Wang Y. Furanodiene, a natural product, inhibits breast cancer growth both in vitro and in vivo. Cell Physiol Biochem 2012; 30: 778-790.
[20] Sun XY, Zheng YP, Lin DH, Zhang H, Zhao F and Yuan CS. Potential anti-cancer activities of Furanodiene, a Sesquiterpene from Curcuma wenyujin. Am J Chin Med 2009; 37: 589-596.
[21] Xu WS, Li T, Wu GS, Dang YY, Hao WH, Chen XP, Lu JJ and Wang YT. Effects of furanodiene on 95-D lung cancer cells: apoptosis, autophagy and G1 phase cell cycle arrest. Am J Chin Med 2014; 42: 243-255.
[22] Zhong ZF, Tan W, Tian K, Yu H, Qiang WA and Wang YT. Combined effects of furanodiene and doxorubicin on the migration and invasion of MDA-MB-231 breast cancer cells in vitro. Oncol Rep 2017; 37: 2016-2024.
[23] Hermes M, Geisler H, Osswald H, Riehle R and Kloor D. Alterations in S-adenosylhomocysteine metabolism decrease O6-methylguanine DNA methyltransferase gene expression without affecting promoter methylation. Biochem Pharmacol 2008; 75: 2100-2111.
[24] Latancia MT, Leandro GDS, Bastos AU, Moreno NC, Ariwoola AA, Martins DJ, Ashton NW, Ribeiro VC, Hoch NC, Rocha CRR, Woodgate R and Menck CFM. Human translesion DNA polymerases iota and kappa mediate tolerance to temozolomide in MGMT-deficient glioblastoma cells. DNA Repair (Amst) 2024; 141: 103715.
[25] Tomar MS, Kumar A, Srivastava C and Shrivastava A. Elucidating the mechanisms of Temozolomide resistance in gliomas and the strate-

gies to overcome the resistance. Biochim Biophys Acta Rev Cancer 2021; 1876: 188616.
[26] Mathur R, Wang Q, Schupp PG, Nikolic A, Hilz S, Hong C, Grishanina NR, Kwok D, Stevers NO, Jin Q, Youngblood MW, Stasiak LA, Hou Y, Wang J, Yamaguchi TN, Lafontaine M, Shai A, Smirnov IV, Solomon DA, Chang SM, Hervey-Jumper SL, Berger MS, Lupo JM, Okada H, Phillips JJ, Boutros PC, Gallo M, Oldham MC, Yue F and Costello JF. Glioblastoma evolution and heterogeneity from a 3D whole-tumor perspective. Cell 2024; 187: 446-463, e416.
[27] Yabo YA, Niclou SP and Golebiewska A. Cancer cell heterogeneity and plasticity: a paradigm shift in glioblastoma. Neuro Oncol 2022; 24: 669-682.
[28] Delgado-Martin B and Medina MA. Advances in the knowledge of the molecular biology of glioblastoma and its impact in patient diagnosis, stratification, and treatment. Adv Sci (Weinh) 2020; 7: 1902971.
[29] Kong Q, Sun F and Chen X. Impact of fixed-dose combination of germacrone, curdione, and furanodiene on breast cancer cell proliferation. Cell J 2013; 15: 160-165.
[30] Zhong ZF, Hoi PM, Wu GS, Xu ZT, Tan W, Chen XP, Cui L, Wu T and Wang YT. Anti-angiogenic effect of furanodiene on HUVECs in vitro and on zebrafish in vivo. J Ethnopharmacol 2012; 141: 721-727.
[31] Xu WS, Dang YY, Guo JJ, Wu GS, Lu JJ, Chen XP and Wang YT. Furanodiene induces endoplasmic reticulum stress and presents antiproliferative activities in lung cancer cells. Evid Based Complement Alternat Med 2012; 2012: 426521.
[32] Zhu XY, Guo DW, Lao QC, Xu YQ, Meng ZK, Xia B, Yang H, Li CQ and Li P. Sensitization and synergistic anti-cancer effects of Furanodiene identified in zebrafish models. Sci Rep 2019; 9: 4541.
[33] Xu WS, Dang YY, Chen XP, Lu JJ and Wang YT. Furanodiene presents synergistic anti-proliferative activity with paclitaxel via altering cell cycle and integrin signaling in 95-D lung cancer cells. Phytother Res 2014; 28: 296-299.
[34] Shaw R, Basu M, Karmakar S and Ghosh MK. MGMT in TMZ-based glioma therapy: multifaceted insights and clinical trial perspectives. Biochim Biophys Acta Mol Cell Res 2024; 1871: 119673.